1000-0569/2014/030(02)-0350-60 *Acta Petrologica Sinica* 岩石学报

Geochemical, Sr-Nd isotope, and zircon U-Pb geochronological constraints on the origin of Early Cretaceous carbonatite dykes, northern Shanxi Province, China

山西省早白垩纪碳酸岩元素同位素和锆石 U-Pb 定年研究*

LIU Shen[1], FENG CaiXia[1], HU RuiZhong[2], LAI ShaoCong[1], COULSON Ian M[3], FENG GuangYing[2] and YANG YuHong[2]

刘燊[1] 冯彩霞[1] 胡瑞忠[2] 赖绍聪[1] Ian M Coulson[3] 冯光英[2] 杨毓红[2]

1. State Key Laboratory of Continental Dynamics and Department of Geology, Northwest University, Xi'an 710069, China
2. State Key Laboratory of Ore Deposit Geochemistry, Institute of Geochemistry, Chinese Academy of Sciences, Guiyang 550002, China
3. Solid Earth Studies Laboratory, Department of Geology, University of Regina, Regina, Saskatchewan, S4S 0A2, Canada
1. 大陆动力学国家重点实验室,西北大学地质学系,西安 710069
2. 矿床地球化学国家重点实验室,中国科学院地球化学研究所,贵阳 550002
3. 固体地球研究实验室,里贾纳大学地质学系,萨斯喀彻 S4S 0A2

Received: 2013-08-05, *Accepted*: 2013-10-25.

Liu S, Feng CX, Hu RZ, Lai SC, Coulson IM, Feng GY and Yang YH. 2014. Geochemical, Sr-Nd isotope, and zircon U-Pb geochronological constraints on the origin of Early Cretaceous carbonatite dykes, northern Shanxi Province, China. *Acta Petrologica Sinica*, 30(2):350 – 360

Abstract Carbonatite dyke swarms are widespread across the North China Craton (NCC) in Shanxi Province. Here, we present new geochemical, Sr-Nd isotope, and U-Pb zircon age data for representative samples of the dykes. Laser ablation-inductively coupled plasma-mass spectrometry (LA-ICP-MS) U-Pb analyses yielded a Cretaceous age of 132.9 ± 0.6Ma for zircons extracted from one dyke. Whole rock K-Ar ages for three samples range from 131.3Ma to 132.6Ma. The carbonatites have highly uniform major element compositions and are enriched in light rare earth elements and large ion lithophile elements (LILEs; e.g., Ba, U, Pb, and Sr), and depleted in K and high field strength elements (HFSEs; e.g., Ta, P, and Ti). The carbonatite dykes have relatively uniform $(^{87}Sr/^{86}Sr)_i$ values that range from 0.7079 to 0.7083, and negative values of $\varepsilon_{Nd}(t)$ (−16.7 to −15.2). These data suggest that the dyke magmas were derived from the partial melting of an enriched region of the lower lithospheric mantle, with evident crustal contamination. The carbonatite dykes within the northern NCC formed during the mixing of the continental crust with sub-continental lithospheric mantle.

Key words Cretaceous; Carbonatite dykes; Shanxi Province; Northern NCC

摘 要 碳酸岩广泛出露在华北克拉通的山西省。此文中,针对研究区的碳酸岩墙,我们给出新的地球化学、Sr-Nd 同位素和锆石 U-Pb 年龄。LA-ICP-MS 锆石定年结果显示,该岩墙的侵位年龄为 132.9Ma,全岩 K-Ar 年龄为 131.3 ~ 132.6 Ma。碳酸岩墙具有非常一致的主量元素组成,富集轻稀土元素和大离子亲石元素(Ba、U、Pb、Sr),以及亏损 K 和高场强元素(Ta、P 和 Ti)。另外,该岩墙具有相对一致的$(^{87}Sr/^{86}Sr)_i$(0.7079 ~ 0.7083)和负的$\varepsilon_{Nd}(t)$(−16.7 ~ −15.2)。以上地球化学特征表明,该岩墙为大陆地壳和此大陆岩石圈地幔混合时期,受明显地壳混染的下岩石圈地幔的部分熔融作用。

关键词 白垩纪;碳酸岩墙;山西;华北克拉通北部

中图法分类号 P588.313; P597.3

* This article was supported by the Opening Project (201206) of the State Key Laboratory of Ore deposit Geochemistry, and National Natural Science Foundation of China (41373028).

Author: Liu Shen, 1974, Professor, is now focused on igneous rocks and geochemistry, E-mail: liushen@vip.gyig.ac.cn, liushen@nwu.edu.cn

1 Introduction

Carbonatite and mafic dykes develop during periods of lithospheric extension (Hall, 1982; Hall and Fahrig, 1987; Tarney and Weaver, 1987; Zhao and McCulloch, 1993; Yan *et al.*, 2007) and have special geochemical features, attracting the attention of geologists' worldwide (Le Bas, 1977; Bell, 1989; Bailey, 1993; Yan *et al.*, 2007). Nowadays, more than 530 known carbonate occurrences have been founded on all continent and at some oceanic localities (e. g., the East African Rift, Kontozero Graben in northwestern Russia, Cape Verde, Canary archipelagos, North and Central Alantic Ocean, the NCC) (Bell and Tilton, 2001; Bell and Rukhlov, 2004; Yan *et al.*, 2007; Doucelance *et al.*, 2010; Rukhlov and Bell, 2010; Xu *et al.*, 2011). Since these rocks are important in understanding the chemical evolution of the mantle over time and assessing continental break-up, carbonatites have been attended closely (e. g., Bailey, 1983; Bell and Blenkinsop, 1989; Bell *et al.*, 1999; Bell and Tilton, 2002; Keppler, 2003; Burke *et al.*, 2003; Rukhlov and Bell, 2010). In addition, there are three principal hypotheses about the origin of the carbonatites (Harmer, 1999; Lee and Wyllie, 1997; Verhulst *et al.*, 2000; Xu *et al.*, 2007). However, there are visible uncertainties on the origin and age dating.

Mafic dykes are widespread throughout the NCC, and more than 600 dykes have been identified within swarms that trend NE-SW, NW-SE, and E-W (Liu *et al.*, 2008a, b, 2009, 2012a, b, 2013). These rocks provide important information on the extensional tectonism of the area, mantle composition, structures, and the nature and evolution of dynamic processes in the NCC. In contrast, carbonatites distribute very little in NCC (Bai and Li, 1985; Ying *et al.*, 2004; Yan *et al.*, 2007), and they are highly Si-undersaturated magma. They are very important for investigation of the extensional history, upper mantle composition, nature, evolution and geodynamic processes of NCC. The carbonatites in NCC were formed mainly at three periods, i. e., Late Paleoproterozoic-Early Mesoproterozoic, early and late Mesozoic. Except the carbonatites in Laiwu and Zibo, other rocks were derived from enriched lithospheric mantle (Yan *et al.*, 2007). Nevertheless, apparent controversy on the dynamic mechanism still extent.

Generally, zircon crystallizes from Si-saturated melt and it is commonly used for U-Pb-Hf-O isotope analyses. However, zircon in carbonatites usually occurs as a xenocryst in carbonatite due to crustal contamination and/or magma mixing (Guo *et al.*, 2013). Thus, we can select enough zircon from carbonatite, and provide precise and convincing U-Pb age.

Accordingly, more investigation on the carbonatite dykes of the NCC is required. Here, we present new zircon U-Pb ages obtained using laser ablation-inductively coupled plasma-mass spectrometry (LA-ICP-MS), as well as new petrological, whole-rock geochemical, and Sr-Nd isotopic data for representative samples of the carbonatite dykes in the northern NCC. These data allow us to constrain the emplacement ages of these dykes and discuss their petrogenesis.

2 Geological setting and petrography

The present study area, located in northern Shanxi Province (Tashan coalmine, Datong), is part of the NCC, the largest and oldest craton in China. The NCC consists of eastern and western blocks of Archean material, and an N-S trending mid-continental orogenic belt of Proterozoic age (Zhao *et al.*, 2001; Fig. 1a). There are numerous carbonatite dykes coexisting with lamprophyre dykes, and all the carbonatites are calcite carbonatites. The country rocks in the study area include Archean leptynites, and Proterozoic, Ordovician, Carboniferous, and Tertiary sedimentary rocks, including limestones (Fig. 1b).

Individual dykes are vertical, trend between NE-SW and N-S, and range from 10m to 30m in width and 150m to 300m in length (Fig. 1b). They intrude Carboniferous coal seams. The carbonatites are mainly composed of calcite ($>$85vol. %) with variable amounts of interstitial apatite and magnetite. A few xenoliths from the coal measures are present in the dykes, and chilled margins can be observed at the dyke edges.

Fresh equigranular carbonatites in the study area are light gray in color, and weathered examples are light brown. Grain sizes range from 0. 8mm to 2. 2mm. Porphyritic carbonatites are dark green in color, and they are sometimes massive, sometimes brecciated. The phenocrysts include phlogopites up to 1. 3cm in size and occasional pyroxenes, and the micro-granular matrix is made up of calcite, olivine, phlogopite, plagioclase, apatite, magnetite, and zircon. The dykes also contain brecciated material of gneiss, limestone, marble, and basalt. The blocks in the breccias range in size from several millimeters to 4. 5cm.

3 Analytical techniques

3. 1 Zircon LA-ICP-MS U-Pb dating

Euhedral zircons were separated from one sample (TX01) using conventional heavy liquid and magnetic techniques at the Langfang Regional Geological Survey, Hebei Province, China. After separation and mounting, the internal and external

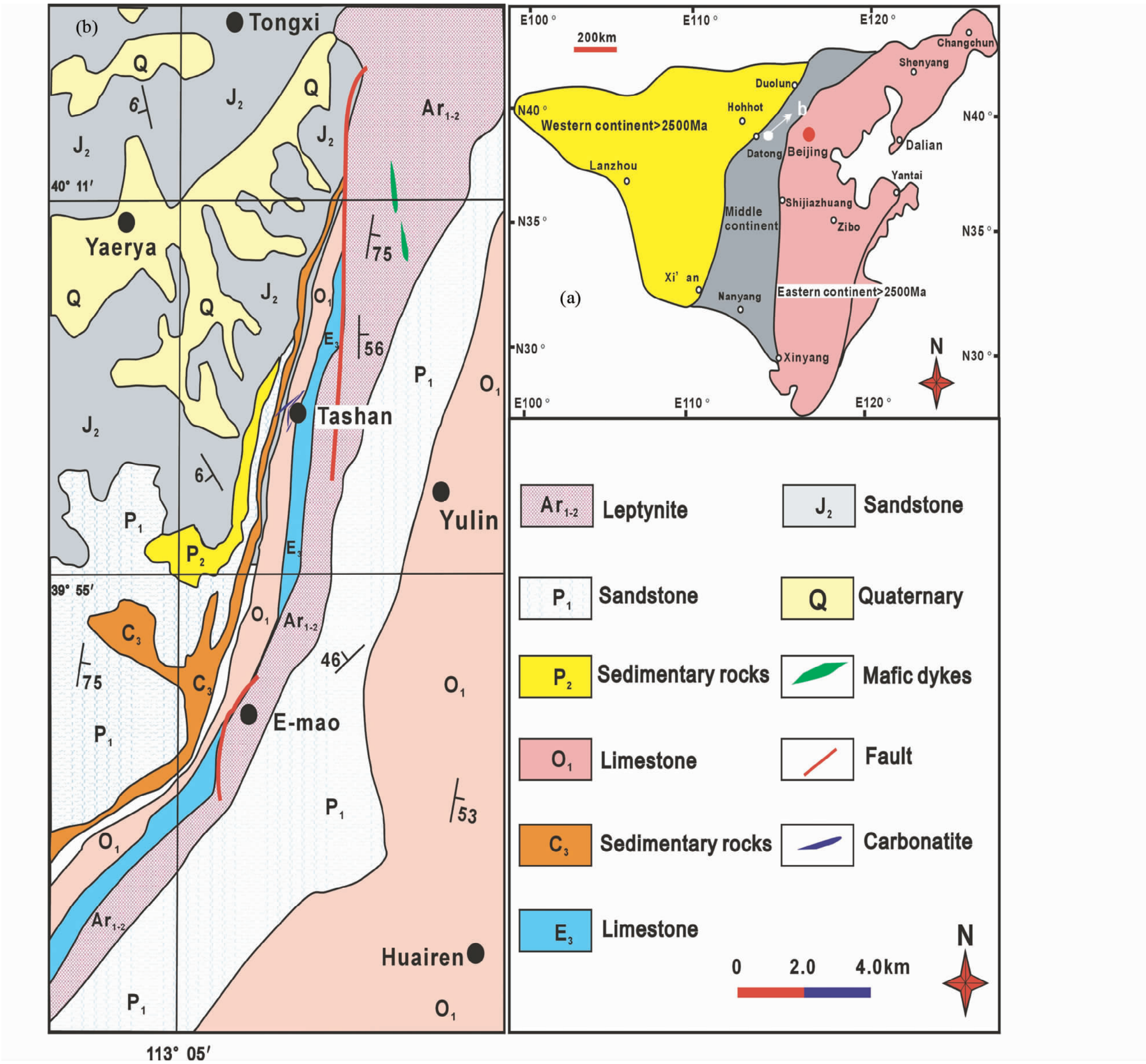

Fig. 1 Study area in China (a) and geological map of the study area, showing the distribution of carbonatite dykes (b)

structures of the zircons were imaged using transmitted light, reflected light, and cathodoluminescence (CL) at the State Key Laboratory of Continental Dynamics, Northwest University, China. Prior to zircon U-Pb dating, the surfaces of grain-mounts were washed in dilute HNO_3 and pure alcohol to remove any potential lead contamination. Zircon U-Pb ages were determined using LA-ICP-MS (Table 1; Fig. 2) and an Agilent 7500a ICP-MS instrument equipped with a 193nm excimer laser at the State Key Laboratory of Geological Processes and Mineral Resources, China University of Geoscience, Wuhan, China. The zircon standard #91500 was used for quality control, and a NIST 610 standard was used for data optimization. A spot diameter of 24m was used during analysis, and we employed the methodology described by Yuan *et al.* (2004) and Liu *et al.* (2010b). Correction for common Pb was undertaken following Andersen (2002), and the resulting data were processed using the GLITTER and ISOPLOT programs (Ludwig, 2003; Table 1; Fig. 2). Uncertainties in the individual LA-ICP-MS analyses are quoted at the 95% (1σ) confidence level.

3.2 Whole-rock K-Ar dating

Fresh samples were selected and crushed to powder, and then K-Ar ages were analyzed at the K-Ar age laboratory of the Institute of Geology, China Seismological Bureau. An MM-1200 mass spectrograph was used for the K-Ar age determination, and its affiliated extraction system is produced by the VG corp. The constants are adopted as $\lambda = 5.543 \times 10^{-10}/a$, $\lambda_e = 0.58 \times 10^{-10}/a$,

Table 1 LA-ICP-MS U-Pb isotope data for zircons from carbonatite dykes of the NCC

TX01 Spot	($\times 10^{-6}$)			Th/U	Isotopic ratios						Age (Ma)					
	Th	U	Pb		$^{207}Pb/^{206}Pb$	1σ	$^{207}Pb/^{235}U$	1σ	$^{206}Pb/^{238}U$	1σ	$^{207}Pb/^{206}Pb$	1σ	$^{207}Pb/^{235}U$	1σ	$^{206}Pb/^{238}U$	1σ
1. 1	382	1509	37	0. 25	0. 0506	0. 0015	0. 1435	0. 0093	0. 0210	0. 0002	222	48	139	4	134	1
2. 1	185	1074	24	0. 17	0. 0510	0. 0021	0. 1444	0. 0094	0. 0210	0. 0002	241	73	140	5	134	2
3. 1	1053	1074	30	0. 98	0. 0496	0. 0017	0. 1442	0. 0088	0. 0211	0. 0002	178	60	137	4	134	1
4. 1	255	1459	33	0. 17	0. 0514	0. 0015	0. 1454	0. 0093	0. 0210	0. 0002	256	46	140	4	134	1
5. 1	301	1666	38	0. 18	0. 0528	0. 0014	0. 1458	0. 0089	0. 0206	0. 0002	321	45	142	3	132	1
6. 1	343	411	11	0. 83	0. 0504	0. 0026	0. 1450	0. 0087	0. 0211	0. 0003	214	96	138	7	134	2
7. 1	399	1792	42	0. 22	0. 0517	0. 0015	0. 1455	0. 0091	0. 0207	0. 0002	271	48	140	4	132	1
8. 1	199	1159	27	0. 17	0. 0468	0. 0016	0. 1451	0. 0088	0. 0206	0. 0002	41	56	127	4	133	1
9. 1	85	80	2. 3	1. 05	0. 0481	0. 0015	0. 1438	0. 0095	0. 0207	0. 0002	102	59	131	4	132	1
10. 1	232	1423	32	0. 16	0. 0513	0. 0013	0. 1456	0. 0094	0. 0208	0. 0002	254	48	139	4	133	1
11. 1	232	238	26	0. 97	0. 0526	0. 0013	0. 1435	0. 0089	0. 0209	0. 0002	312	39	141	3	133	1
12. 1	185	1336	31	0. 14	0. 4750	0. 0015	0. 1443	0. 0086	0. 0205	0. 0002	4165	39	128	4	132	1

Table 2 Whole-rock K-Ar ages of the studied carbonatites

Sample No.	Rock type	Dating method	K(%)	$^{40}Ar_{rad}$ (mol/g)	$^{40}Ar_{rad}$ (%)	Age(Ma ± 1σ)
TX-3			1. 76	4.31×10^{-6}	95. 03	131. 3 ± 2. 4
TX-6	carbonatite	Whole rock (K-Ar)	2. 25	5.48×10^{-6}	86. 66	132. 5 ± 2. 7
TX-12			1. 55	3.66×10^{-6}	93. 08	132. 6 ± 2. 5

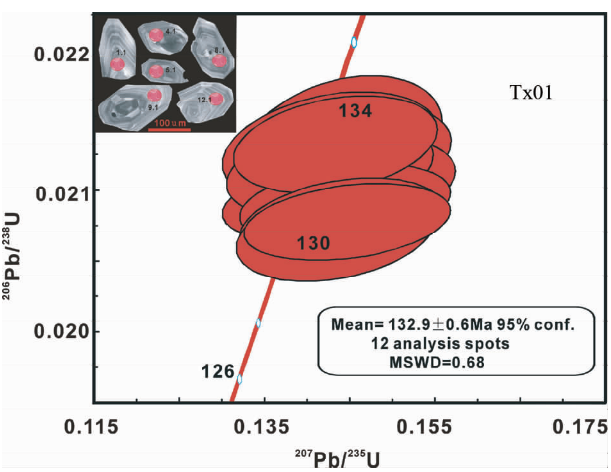

Fig. 2 Zircon LA-ICP-MS U-Pb concordia diagrams and CL images of zircons separated from dykes of carbonatite in the northern NCC, China

$\lambda_\beta = 0.58 \times 10^{-10}/a$, $^{40}K/^{38}K = 1.167 \times 10^{-4}/mol/g$ (Table 2).

3.3 Whole-rock geochemistry and Sr-Nd isotope analyses

Whole rock samples were trimmed to remove altered surfaces, and fresh portions were collected and then powdered in an agate mill to about 200 meshes for analyses of isotopes, and major and trace elements.

Major element contents were determined in fused glass discs using a PANalytical Axios-advance (Axios PW4400) X-ray fluorescence spectrometer (XRF) at the State Key Laboratory of Ore Deposit Geochemistry, Institute of Geochemistry, Chinese Academy of Sciences, Guiyang, China. These analyses have a precision of < 5% (Table 3). Loss on ignition (LOI) values was obtained using 1g of powder heated to 1100℃ for 1 hour. Trace element concentrations were determined using ICP-MS at the State Key Laboratory of Ore Deposit Geochemistry, Institute of Geochemistry, Chinese Academy of Sciences, Guiyang, China, using the procedures outlined in Qi *et al.* (2000), and the analytical uncertainty is ±5% (Table 4). Sample powders used for Rb-Sr and Sm-Nd isotope analyses were spiked with mixed isotope tracers, dissolved in Teflon capsules with HF and HNO_3 acids, and separated by conventional cation-exchange techniques. Isotopic measurements were performed using a Finnigan Triton Ti thermal ionization mass spectrometer at the State Key Laboratory of Geological Processes and Mineral Resources, China University of Geosciences, Wuhan, China. Procedural blanks yielded concentrations of < 200pg for Sm and Nd, and < 500pg for Rb and Sr. Mass fractionation corrections for Sr and Nd isotopic ratios were based on $^{86}Sr/^{88}Sr = 0.1194$ and $^{146}Nd/^{144}Nd = 0.7219$, respectively, and analyses of the NBS987 and La Jolla standards yielded values of $^{87}Sr/^{86}Sr = 0.710246 \pm 16$ (2σ) and $^{143}Nd/^{144}Nd = 0.511863 \pm 8$ (2σ), respectively (Table 5).

Table 3 Major element contents (wt%) for the carbonatite dykes of the NCC

Sample	SiO_2	Al_2O_3	$Fe_2O_3{}^T$	MgO	CaO	Na_2O	K_2O	MnO	P_2O_5	TiO_2	LOI
TX-1	20.37	11.35	6.32	1.93	28.40	0.37	2.76	0.14	1.26	1.06	27.60
TX-2	21.84	10.87	4.84	0.83	29.70	0.14	2.53	0.13	1.31	1.05	26.80
TX-3	20.65	11.18	3.87	1.27	29.60	0.13	2.49	0.11	1.28	1.01	27.10
TX-4	21.74	11.12	4.63	1.00	27.90	0.20	2.55	0.13	1.27	1.06	26.90
TX-5	20.53	11.48	3.20	0.35	30.10	0.52	2.34	0.12	1.27	1.07	27.69
TX-6	20.75	11.25	4.24	0.65	28.73	0.28	2.71	0.12	1.30	1.05	26.48
TX-7	19.31	10.93	7.89	2.36	22.42	0.36	2.80	0.17	1.37	1.06	32.73
TX-8	20.69	11.62	3.42	0.77	30.12	0.14	2.63	0.11	1.28	1.05	27.31
TX-9	19.70	11.73	2.57	0.38	31.64	0.07	2.26	0.10	1.31	1.06	28.00
TX-10	21.25	10.82	4.91	0.96	28.27	0.09	2.55	0.14	1.29	1.04	26.96
TX-11	19.46	10.84	7.83	2.37	22.38	0.35	2.83	0.16	1.39	1.05	31.66
TX-12	20.78	11.22	4.23	0.63	27.76	0.25	2.63	0.11	1.28	1.04	30.62
TX-13	20.55	11.43	3.16	0.33	29.86	0.47	2.31	0.11	1.25	1.06	28.65
TX-14	21.66	11.08	4.57	0.98	27.84	0.22	2.54	0.13	1.26	1.08	28.16
TX-15	19.67	11.65	2.53	0.36	31.71	0.06	2.22	0.12	1.28	1.07	29.12

Note: LOI = loss on ignition. Total iron is expressed as $Fe_2O_3{}^T$

Table 4 Trace element compositions ($\times 10^{-6}$) of the carbonatite dyke within the NCC

Sample	TX-1	TX-2	TX-3	TX-4	TX-5	TX-6	TX-7	TX-8	TX-9	TX-10	TX-11	TX-12	TX-13	TX-14	TX-15
Sc	12.9	12.8	13.0	13.4	12.8	14.5	23.1	13.7	13.4	14.1	12.6	12.8	13.3	13.6	14.3
V	169	165	165	175	171	164	203	164	161	186	168	163	181	173	171
Cr	338	348	347	373	365	356	414	353	371	394	326	351	366	262	367
Ni	37.7	36.7	41.1	39.0	37.2	42.6	46.5	29.3	30.9	40.0	37.4	37.3	41.6	30.4	41.8
Rb	36.3	24.8	28.1	33.4	29.5	36.3	38.9	38.7	32.0	35.6	36.5	24.5	32.7	38.6	36.5
Sr	978	956	980	995	1020	1010	1090	1140	1060	1040	986	961	988	1125	1016
Y	28.2	32.2	30.7	27.7	33.3	27.9	33.5	30.0	31.4	28.2	27.6	31.9	26.9	29.5	28.2
Zr	300	261	273	264	271	270	342	279	284	278	304	264	268	283	265
Nb	9.39	9.48	9.48	9.48	9.57	9.48	10.10	9.12	9.21	9.39	9.38	9.53	9.37	9.13	9.32
Ba	3220	2550	2670	3140	2050	2850	3950	2730	2630	3010	3190	2489	3132	2693	2839
La	41.1	39.6	41.5	38.0	40.0	39.7	40.7	43.6	42.4	39.3	41.7	38.7	37.5	43.5	38.9
Ce	82.0	81.7	83.9	77.7	79.6	78.4	81.3	82.3	81.8	77.2	84.2	82.5	78.3	81.6	78.2
Pr	10.6	10.8	10.8	10.2	10.7	10.1	10.9	10.8	10.9	10.3	10.5	11.3	11.1	10.4	10.3
Nd	43.6	45.3	45.8	43.4	44.8	42.6	46.3	43.1	46.5	43.0	44.5	46.2	42.5	42.3	43.2
Sm	8.31	9.13	9.20	8.88	9.20	8.50	9.39	9.18	9.34	9.04	8.42	9.22	8.93	9.22	8.38
Eu	2.47	2.55	2.61	2.56	2.68	2.50	2.88	2.60	2.58	2.59	2.43	2.48	2.54	2.57	2.44
Gd	7.80	8.14	8.51	7.83	8.44	7.27	8.33	7.62	8.35	7.85	8.23	8.16	7.69	8.13	7.16
Tb	0.977	1.030	1.060	1.04	1.13	1.00	1.13	1.01	1.09	1.00	1.02	1.04	1.06	1.02	0.96
Dy	4.60	5.00	4.91	4.42	5.19	4.43	5.04	4.48	4.85	4.46	4.62	5.05	4.46	4.52	4.36
Ho	0.96	1.02	1.03	0.92	1.12	0.87	1.09	0.96	0.98	0.92	0.98	1.03	0.94	0.98	0.82
Er	2.56	2.72	2.70	2.47	2.97	2.48	2.88	2.57	2.58	2.57	2.54	2.74	2.49	2.49	2.37
Tm	0.36	0.38	0.36	0.32	0.41	0.31	0.36	0.32	0.35	0.31	0.35	0.37	0.31	0.32	0.31
Yb	2.29	2.41	2.39	2.10	2.61	2.10	2.37	2.24	2.29	2.12	2.27	2.45	2.14	2.26	1.98
Lu	0.33	0.38	0.36	0.31	0.36	0.33	0.33	0.31	0.32	0.29	0.32	0.42	0.28	0.33	0.32
Hf	6.78	6.90	6.80	6.48	7.10	6.74	6.86	6.52	6.48	6.04	6.84	6.95	6.51	6.53	6.56
Ta	0.33	0.34	0.34	0.35	0.36	0.34	0.32	0.31	0.30	0.32	0.35	0.36	0.36	0.34	0.36
Pb	23.4	10.3	16.5	24.2	21.2	24.7	19.7	16.2	13.2	24.3	23.6	10.7	23.8	16.4	25.1
Th	4.20	3.91	4.23	4.18	4.27	4.22	4.97	3.84	3.82	4.03	4.18	3.96	4.19	3.78	4.26
U	0.61	0.79	0.84	0.76	0.66	0.57	1.33	0.75	0.78	0.71	0.63	0.78	0.75	0.79	0.59

Table 5 Sr-Nd isotopic compositions of the carbonatite dykes within the northern NCC

Sample	Sm ($\times10^{-6}$)	Nd ($\times10^{-6}$)	Rb ($\times10^{-6}$)	Sr ($\times10^{-6}$)	$\frac{^{87}Rb}{^{86}Sr}$	$\frac{^{87}Sr}{^{86}Sr}$	2σ	$\left(\frac{^{87}Sr}{^{86}Sr}\right)_i$	$\frac{^{147}Sm}{^{144}Nd}$	$\frac{^{143}Nd}{^{144}Nd}$	2σ	$\left(\frac{^{143}Nd}{^{144}Nd}\right)_i$	$\varepsilon_{Nd}(t)$
TX1	8.31	43.6	36.3	978	0.1073	0.708317	10	0.708114	0.1152	0.511788	8	0.511688	-15.2
TX2	9.13	45.3	24.8	956	0.0750	0.708147	10	0.708005	0.1218	0.511774	10	0.511668	-15.6
TX3	9.20	45.8	28.1	980	0.0829	0.708143	12	0.707986	0.1214	0.511752	9	0.511646	-16.0
TX4	8.88	43.4	33.4	995	0.0970	0.708204	10	0.708021	0.1237	0.511742	10	0.511634	-16.2
TX5	9.20	44.8	29.5	1020	0.0836	0.708013	10	0.707855	0.1241	0.511739	8	0.511631	-16.3
TX6	8.50	42.6	36.3	1010	0.1039	0.708245	12	0.708049	0.1206	0.511716	9	0.511611	-16.7
TX7	9.39	46.3	38.9	1090	0.1031	0.708268	10	0.708073	0.1226	0.511722	10	0.511615	-16.6
TX8	9.18	43.1	38.7	1140	0.0981	0.708477	12	0.708292	0.1288	0.511774	10	0.511662	-15.7
TX9	9.34	46.5	32.0	1060	0.0872	0.708284	10	0.708119	0.1214	0.511724	8	0.511618	-16.6
TX10	9.04	43.0	35.6	1040	0.0989	0.708267	10	0.708080	0.1271	0.511738	9	0.511627	-16.4

Note: using Chondrite Uniform Reservoir (CHUR) values, and decay constants of $\lambda_{Rb}=1.42\times10^{-11}$ $year^{-1}$ (Steiger and Jäger, 1977) and $\lambda_{Sm}=6.54\times10^{-12}$ $year^{-1}$ (Lugmair and Harti, 1978)

4 Results

4.1 Zircon U-Pb ages

Euhedral zircons in sample TX01 are clear and prismatic, and have oscillatory magmatic zoning (Fig. 2). Twelve zircons from sample TX01 yielded a weighted mean $^{206}Pb/^{238}U$ age of 132.9 ± 0.6Ma (1σ, 95% confidence interval; Table 1; Fig. 2). These new data provide the best estimates of carbonate dyke crystallization ages in the study area, and no inherited zircons were observed in either sample population.

4.2 Whole-rock K-Ar ages

The K-Ar dating results are listed in Table 2. The results show that the ages of three carbonatites range from 131.3 ± 2.4Ma to 132.6 ± 2.6Ma, implying that the studied carbonatites were the products of early Cretaceous magmatism.

4.3 Major and trace elements

The results of major and trace element analyses of the studied carbonatites are presented in Table 3 and Table 4. In a CaO-MgO-($Fe_2O_3^T$ + MnO) classification diagram (Fig. 3), all samples except two fall into the field of ferro-carbonatite, and the other two carbonatites straddle the region of calico-carbonatite.

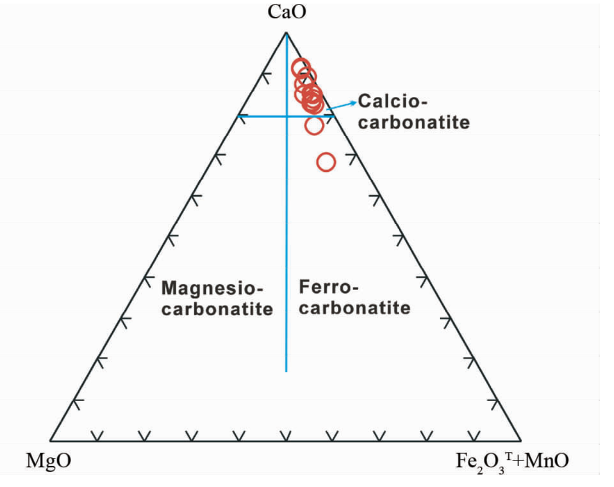

Fig. 3 Plot of the studied carbonatites on the CaO-MgO-($Fe_2O_3^T$ + MnO) classification diagram (after Woolley and Kempe, 1989)

The high SiO_2 content (19.31% ~ 21.84%) of the studied carbonatites is reflected in the presence of phlogopite phenocrysts (Ying *et al.*, 2004), and the carbonatites have steep rare earth element (REE) patterns, indicating an enriched source (Ying *et al.*, 2004). Carbonatites generally contain more REEs and have higher ratios of light RREs to heavy REEs than any other igneous rocks (Woolley and Kempe, 1989; Hornig-Kjarsgaard, 1998). However, Fig. 4a shows that the chondrite normalized REE patterns for the NCC carbonatites studied by us (with very small REE (86×10^{-6} ~ 178×10^{-6}) and steeper REE patterns) are very different from those of most carbonatites worldwide (Table 3; Woolley and Kempe, 1989). In the primitive-mantle-normalized diagrams (Fig. 4b), the NCC carbonatites are enriched in Ba, Th, Sr, and U, and markedly depleted in Rb, K, and Ti, and this is in common with carbonatites elsewhere (Nelson *et al.*, 1988; Woolley and Kempe, 1989). The Nb/Ta and Zr/Hf ratios in the studied rocks are 26 ~ 32 and 38 ~ 50, respectively, almost comparable with ratios of 17 and 36 in primitive mantle and OIB (Sun and McDonough, 1989), and consistent with most carbonatites elsewhere, as summarized by Thompson *et al.* (2002). The Sr and Nd isotope data of the carbonatites are listed in Table 5 and plotted on Fig. 5. All samples have relatively high and uniform initial $^{87}Sr/^{86}Sr$ ratios

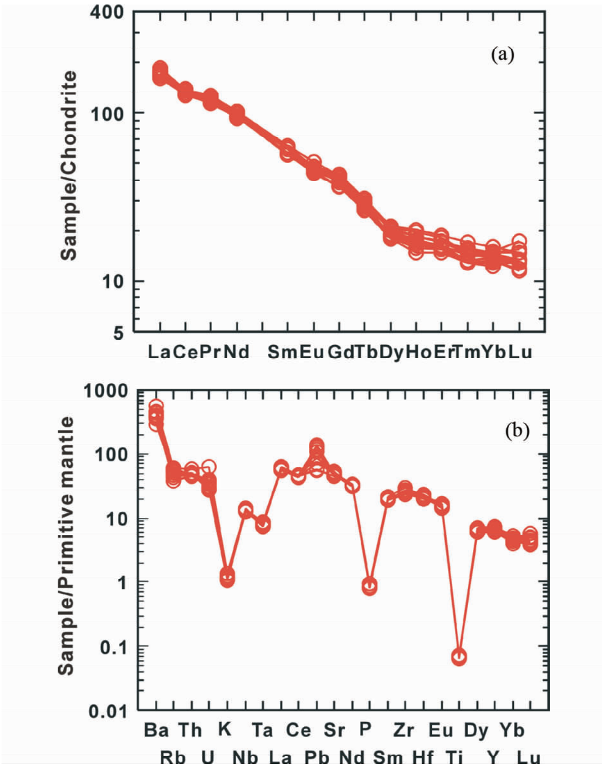

Fig. 4 Chondrite-normalized REE diagram (a, normalization values after Anders and Grevesse, 1989) and primitive-mantle-normalized incompatible element distribution diagram (b, normalization values after Sun and McDonough, 1989) for the carbonatite dykes of the northern NCC, China

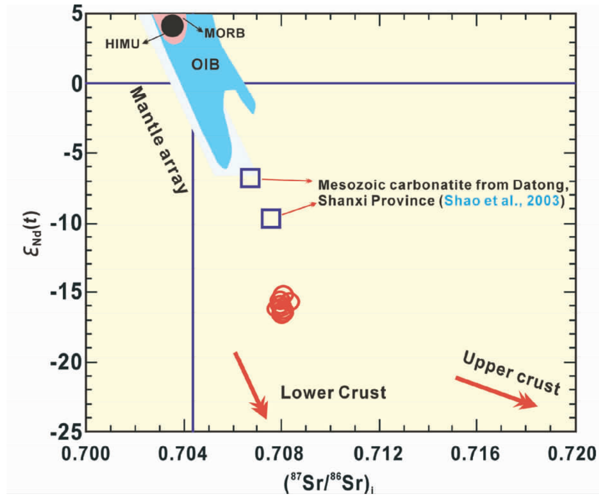

Fig. 5 Variations in initial $^{87}Sr/^{86}Sr$ ratios vs. $\varepsilon_{Nd}(t)$ values for the carbonatite dykes of the northern NCC, China

(0.70798 ~ 0.70829), low $^{143}Nd/^{144}Nd$ ratios (0.51161 ~ 0.51169), and consequently low $\varepsilon_{Nd}(t)$ values (from −16.7 to −15.2). In a plot of $(^{87}Sr/^{86}Sr)_i$ vs. $\varepsilon_{Nd}(t)$, the data from the carbonatites fall in the enriched quadrant (Fig. 5), and this illustrates the sharp contrast between the Sr and Nd isotopic data from the NCC Datong carbonatites and the data from other carbonatites elsewhere (e. g., at E'maokou; Shao *et al.*, 2003).

MORB and OIB data are from Zhang *et al.* (2002), and the mantle array is from Zhang *et al.* (2005)

5 Discussion

5.1 Evidence of a magmatic origin of the NCC carbonatites

The occurrence of carbonatites as dykes, sills, and breccia pipes, as well as the clear-cut contact zones with the country rocks, lends overall support to a magmatic origin for the studied carbonatites rather than remobilized limestones. Major element chemistry also provides clear evidence that the studied carbonatites are magmatic and not simply derived from sedimentary limestones or metamorphic marbles. For instance, the carbonatites have much higher SiO_2 concentrations (19.31% ~ 21.84%, Table 3) than those of limestones. The REE distribution patterns and trace element spidergrams for the studied carbonatites are similar to those for known carbonatites, and are different from those of limestone (Le Bas *et al.*, 2002; Ying *et al.*, 2004). In summary, all the evidence points convincingly to a magmatic origin for the studied carbonatites.

5.2 Mantle source

The carbonatite and mafic dykes are both associated with lithospheric extension, and the fact that the studied carbonatites coexist with many other contemporaneous mafic dykes suggests they may all have a similar source (possibly the lithospheric mantle). Generally, the carbonatites are enriched in incompatible elements (Ba, Th, Sr, and U), implying they were derived by a low degree of partial melting of the mantle (Shao *et al.*, 2003). As mentioned above, a striking feature of the studied carbonatites is their very negative $\varepsilon_{Nd}(t)$ values (from −16.7 to −15.2), and this, coupled with the extremely high initial $^{87}Sr/^{86}Sr$ ratios (0.70798 ~ 0.70829), obviously excludes the possibility that their primary isotopic ratios have been changed by the large assimilation of crustal materials (Shao and Zhang, 2002; Ying *et al.*, 2004). Although some carbonatites include crustal breccias and xenoliths, their Sr and Nd isotopic ratios are quite similar to those of the carbonatites that are relatively pure and lacking crustal breccias (Ying *et al.*, 2004). To summarize, the Sr-Nd isotopic ratios in the carbonatites studied indicate derivation from an enriched lower lithospheric mantle source.

5.3 Crustal contamination

As mentioned above, the extremely high abundances of Sr and Nd in carbonatites can buffer their primary isotopic ratios against crustal contamination during ascent of the magma, which is further supported by the absence of any inherited zircons. However, the fact that the carbonatites studied here are characterized by high Sr isotope ratios and negative $\varepsilon_{Nd}(t)$ values suggests that the magmas might have assimilated significant amounts of crustal material. Furthermore, it is generally accepted that the carbonatites will be depleted in Zr, Hf, Nb, Ta and Ti. However, the studied carbonatite dykes almost show no Zr-Hf depletion with respect to neighboring Sm and Eu. Implying these carbonatite dykes experienced contamination or AFC processes by zircon-rich crustal rocks such as the wall granitic rocks, and the contaminated magmas would not show Zr-Hf depletion of the primary carbonatitic melts. In summary, there exists a certain amount of crustal contamination during magma ascending.

5.4 Genetic processes

The carbonatites in NCC are widespread in Henan Province (Fangcheng), Hebei Province (Huai'an and Zhuolu), Shanxi Province (Huairen and Zijinshan), Shaanxi Province (Huayin and Luonan) and Inner Mongolia Autonomous Region (Banyan Obo and Fengzhen), however, the majority of the carbonatites distribute in the north and south margin of the NCC. In addition, in central and eastern NCC, carbonatites only were found in Zijinshan (Shanxi Province) and Laiwu-Zibo (Shandong Province) (Yan *et al.*, 2007). The main types of the carbonatite are calcite carbonatite, and most of them are paragenetic with alkaline rocks. Furthermore, the age of the carbonatites in NCC has a wide distribution, i.e., Paleoproterozoic (~1.8Ga), Mesoproterozoic (1.7~1.2Ga), Neoproterozoic (786Ma), Early Paleozoic (433Ma), Early Mesozoic (239~204Ma), and Late Mesozoic (132~124Ma) (Bai and Yuan, 1985; Yan *et al.*, 2007; Mu and Yan, 1992; Qiu *et al.*, 1993; Ren *et al.*, 1999; Zou *et al.*, 2000; Ying and Zhou, 2001; Shao *et al.*, 2003; Fan *et al.*, 2006; Yang *et al.*, 2006). According to previous research, the carbonatites in NCC, especially during the Late Triassic, were considered to be related with extension due to crust rifting (Mu and Yan, 1992; Mu *et al.*, 2001), the subduction between Qinling Plate and the NCC (Ren *et al.*, 1999), the control of different structure (Shao *et al.*, 2003), and the subduction between paleoasian ocean plate, Yangtze Craton and the NCC (Yan *et al.*, 2007). In addition to carbonatites, there are also other extension-derived rocks in NCC, such as alkaline rocks (Mu and Yan, 1992) and mafic dykes (Shao and Zhang, 2002; Shao *et al.*, 2003; Yang *et al.*, 2004; Hou *et al.*, 2006, 2008; John *et al.*, 2010; Li *et al.*, 2010; Peng, 2010; Peng *et al.*, 2005, 2007, 2008, 2010, 2011a, b; Liu *et al.*, 2006, 2008a, b, 2009, 2012a, b, 2013).

Hence, the genetic processes of the studied carbonatites should be discussed. There are currently three representative models for the origin of carbonatites: 1) direct partial melting (< 1.0%) of asthenospheric or lithospheric mantle; 2) fractional crystallization of nepheline magma; and 3) liquation (Shao *et al.*, 2003). With respect to the studied carbonatites, we note that feldspars and micas are visible in the carbonatites, and that the carbonatites are characterized by high contents of Cr and Ni, and low contents of Nb and Ta. These observations indicate that the carbonatites were formed by liquation. However, a dynamic model is required to further decipher the origin of these rocks.

Geophysical evidence suggests that the Datong area is in a special tectonic location of apparent asthenospheric upwelling and lithospheric thinning. In the Mesozoic, following the collision of the NCC with various other continental blocks (e.g., the Siberia Block), and after the closure of the ancient Pacific/Tethys Ocean, the regional stresses were reduced, and the NCC underwent a transformation in tectonic regime from compression to extension (Zhai *et al.*, 2004). This resulted in large-scale uplift of the deep mantle, as well as considerable extension of the crust, and the widely distributed extension-derived igneous rocks, including numerous mafic, alkaline, and carbonatite dykes in the NCC, have been extensively studied (Wu, 1966; He *et al.*, 1986; Zhang, 1993; Shao and Zhang, 2002; Chen and Zhai, 2003; Shao *et al.*, 2003, 2005; Yang *et al.*, 2004; Liu *et al.*, 2005, 2006, 2008a, b, 2009, 2010a, 2011, 2012a, b, 2013; Yan *et al.*, 2007; Zhang, 2007; Feng *et al.*, 2010, 2012). This may be the tectonic context in which the carbonatite dykes in the study area were formed.

Based on the description above, the studied carbonatites are characterized by enrichment in LILE (e.g., Ba, Th, Sr, U) and LREE, depletion in HREE and HFSE (e.g., Ta, P, Ti), radiogenic isotopes (e.g., Sr and Nd), and contamination by obvious crust materials. It is generally accepted that hydrous melts from the subducting continental crust are commonly of felsic composition. They have principally inherited the continental crust-like signatures of trace elements and radiogenic isotopes (Zheng, 2012). As a result, the mixing of the continental crust with sub-continental lithospheric mantle will result in the above characteristics. Likewise, this can give a reasonable interpretation for the existent crust contamination.

6 Conclusions

The geochronological, geochemical, Sr-Nd isotopic and whole-rocks K-Ar data presented here have allowed the following conclusions to be drawn:

(1) Zircon LA-ICP-MS U-Pb and whole-rock K-Ar dating of carbonate dykes in Shanxi Province, China, indicates the Early Cretaceous (131.3 ± 2.4Ma ~ 132.9 ± 0.6Ma) ages of crystallization.

(2) These carbonate dykes were derived from partial melting of an enriched lower lithospheric mantle source, emplacement of the carbonatite dykes was accompanied with apparent crustal contamination. The carbonatite dykes within the northern NCC formed during the mixing of the continental crust with sub-continental lithospheric mantle.

Acknowledgements The authors thank Lian Zhou and Zhaochu Hu for assistance during zircon U-Pb dating, Sr-Nd isotope, and Hf isotopic analyses.

References

Anders E and Grevesse N. 1989. Abundances of the elements: Meteoritic and solar. Geochimica et Cosmochimica Acta, 53(1): 197 – 214

Andersen T. 2002. Correction of common lead in U-Pb analyses that do not report ^{204}Pb. Chemical Geology, 192(1 – 2): 59 – 79

Bai G and Yuan ZX. 1985. Carbonatite and related mineral deposits. Bulletin of the Institute of Mineral Deposits, Chinese Academy of Geological Sciences, 1: 99 – 175 (in Chinese with English abstract)

Bailey DK. 1983. The chemical and thermal evolution of rifts. Tectonophysics, 94(1 – 4): 585 – 597

Bailey DK. 1993. Carbonate magmas. Journal of the Geological Society, 150(4): 637 – 651

Bell K. 1989. Carbonatites: Genesis and Evolution. London: Unwin Hyman

Bell K and Blenkinsop J. 1989. Neodymium and strontium isotope geochemistry of carbonatites. In: Bell K (ed.). Carbonatites: Genesis and Evolution. London: Unwin Hyman, 278 – 300

Bell K, Kjarsgaard BA and Simonetti A. 1999. Carbonatites-into the twenty-first century. Journal of Petrology, 39: 1839 – 1845

Bell K and Tilton GR. 2001. Nd, Pb, and Sr isotopic compositions of East African cabonatites: Evidence for mantle mixing and plume inhomogeneity. Journal of Petrology, 42(10): 1927 – 1945

Bell K and Tilton GR. 2002. Probing the mantle: The story from carbonatites. EOS. Transactions of the American Geophysical Union, 83(25): 273 – 277

Bell K and Rukhlov AS. 2004. Carbonatites from the Kola alkaline province: Origin, evolution and source characteristics. In: Wall F and Zaitsev AN (eds.). Phoscorites and Carbonatites from Mantle to Mine: The Key Example of the Kola Alkaline. London: Mineralogical Society Series, 10: 421 – 455

Burke K, Ashwal LD and Webb SJ. 2003. New way to map old sutures using deformed alkaline rocks and carbonatites. Geology, 31(5): 391 – 394

Chen B and Zhai MG. 2003. Geochemistry of Late Mesozoic lamprophyre dykes from the Taihang Mountains, North China, and implications for the sub-continental lithospheric mantle. Geological Magazine, 140(1): 87 – 93

Doucelance R, Hammouda T, Moreira M and Martins J. 2010. Geochemical constraints on depth of origin of oceanic carbonatites: The Cape Verde case. Geochimica et Cosmochimica Acta, 74(24): 7261 – 7282

Fan HR, Hu FF, Chen FK, Yang KF and Wang KY. 2006. Intrusive age of No.1 carbonatite dyke from Bayan Obo REE-Nb-Fe deposit, Inner Mongalia: With answers to comment of Dr. Le Bas. Acta Petrologica Sinica, 22(2): 519 – 520 (in Chinese with English abstract)

Feng GY, Liu S, Zhong H, Jia DC, Qi YQ, Wang T and Yang YH. 2010. Geochemical characteristics and petrogenesis of Late Paleozoic mafic rocks from Yumuchuan, Jilin Province. Geochimica, 39(5): 427 – 438 (in Chinese with English abstract)

Feng GY, Liu S, Zhong H, Feng CX, Coulson IM, Qi YQ, Yang YH and Yang CG. 2012. U-Pb zircon geochronology, geochemical, and Sr-Nd isotopic constraints on the age and origin of basaltic porphyries from western Liaoning Province, China. International Geology Review, 54(9): 1052 – 1070

Guo F, Guo JT, Wang CY, Fan WM, Li CW, Zhao L, Li HX and Li JY. 2013. Formation of mafic magmas through lower crustal AFC processes: An example from the Jinan gabbroic intrusion in the North China Block. Lithos, 179: 157 – 174

Hall HC. 1982. The importance and potential of mafic dyke swarms in studies of geodynamic process. Geoscience Canada, 9(3); 145 – 154

Hall HC and Fahrig WF. 1987. Mafic dyke swarms. Geological Association of Canada Special Paper, 34: 1 – 503

Harmer RE. 1999. The petrogenetic association of carbonatite and alkaline magmatism: Constraints from the Spitskop complex, South Africa. Journal of Petrology, 40(4): 525 – 548

He GZ, Shangguan ZG and Zhao YL. 1986. Carbonatites and their patterns of REE distribution in Erdaobian and Boshan areas, China. In: Kimberlite and Related Rocks. 39 – 41

Hornig-Kjarsgaard I. 1998. Rare earth elements in sovitic carbonatites and their mineral phases. Journal of Petrology, 39: 2105 – 2121

Hou GT, Liu YL and Li JH. 2006. Evidence for 1.8Ga extension of the Eastern Block of the North China Craton from SHRIMP U-Pb dating of mafic dyke swarms in Shandong Province. Journal of Asian Earth Sciences, 27(4): 392 – 401

Hou GT, Santosh M, Qian XL, Lister GS and Li JH. 2008. Configuration of the Late Paleoproterozoic supercontinent Columbia: Insights from radiating mafic dyke swarms. Gondwana Research, 14(3): 395 – 409

John DAP, Zhang JS, Huang BC and Andrew PR. 2010. Alaeomagnetism of Precambrian dyke swarms in the North China Shield: The 1.8Ga LIP event and crustal consolidation in Late Palaeoproterozoic times. Journal of Asian Earth Sciences, 41(6): 504 – 524

Keppler H. 2003. Water solubility in carbonatite melts. American Mineralogist, 88(11 – 12): 1822 – 1824

Le Bas MJ. 1977. Carbonatite-Nephelinite Volcanism. London: Wildy & Sons

Le Bas MJ, Subbarao KV and Walsh JN. 2002. Metacarbonatite or marble? The case of the carbonate, pyroxenite, calcite-apatite rock complex at Borra, Eastern Ghats, India. Journal of Asian Earth Sciences, 20(2): 127 – 140

Lee WJ and Wyllie PJ. 1997. Liquid immiscibility between nephelinite and carbonatite from 1.0 to 2.5 Gpa compared with mantle composition. Contributions to Mineralogy and Petrology, 127(1 – 2): 1 – 6

Li TS, Zhai MG, Peng P, Chen L and Guo JH. 2010. Ca. 2.5 billion year old coeval ultramafic-mafic and syenitic dykes in eastern Hebei: Implications for cratonization of the North China Craton. Precambrian

Research, 180(3): 143-155

Liu S, Hu RZ, Zhao JH, Feng CX, Zhong H, Cao JJ and Shi DN. 2005. Geochemical characteristics and petrogenetic investigation of the Late Mesozoic lamprophyres of Jiaobei, Shandong Province. Acta Petrologica Sinica, 21(3): 947-958 (in Chinese with English abstract)

Liu S, Zou HB, Hu RZ, Zhao JH and Feng CX. 2006. Mesozoic mafic dykes from the Shandong Peninsula, North China Craton: Petrogenesis and tectonic implications. Geochemical Journal, 40(2): 181-195

Liu S, Hu RZ, Gao S, Feng CX, Qi L, Zhong H, Xiao T, Qi YQ, Wang T and Coulson IM. 2008a. Zircon U-Pb geochronology and major, trace elemental and Sr-Nd-Pb isotopic geochemistry of mafic dykes in western Shandong Province, East China: Constrains on their petrogenesis and geodynamic significance. Chemical Geology, 255(3-4): 329-345

Liu S, Hu RZ, Gao S, Feng CX, Qi YQ, Wang T, Feng GY and Coulson IM. 2008b. U-Pb zircon age, geochemical and Sr-Nd-Pb-Hf isotopic constraints on age and origin of alkaline intrusions and associated mafic dykes from Sulu orogenic belt, Eastern China. Lithos, 106(3-4): 365-379

Liu S, Hu RZ, Gao S, Feng C, Yu BB, Feng GY, Qi YQ, Wang T and Coulson IM. 2009. Petrogenesis of Late Mesozoic mafic dykes in the Jiaodong Peninsula, eastern North China Craton and implications for the foundering of lower crust. Lithos, 113(3-4): 621-639

Liu S, Hu RZ, Feng GY, Yang YH, Feng CX, Qi YQ and Wang T. 2010a. Distribution and significance of the mafic dyke swarms since Mesozoic in North China Craton. Geological Bulletin of China, 29(2-3): 259-267 (in Chinese with English abstract)

Liu S, Hu RZ, Gao S, Feng CX, Zhong H, Qi YQ, Wang T, Feng GY and Yang YH. 2011. U-Pb zircon age along with geochemical and Sr-Nd-Pb isotopic constraints on the dating and origin of intrusive complexes from the Sulu orogenic belt, eastern China. International Geology Review, 53(1): 61-83

Liu S, Hu RZ, Gao S, Feng CX, Feng GY, Qi YQ, Coulson IM, Yang YH, Yang CG and Tang L. 2012a. Geochemical and isotopic constraints on the age and origin of mafic dykes from eastern Shandong Province, eastern North China Craton. International Geology Review, 54(12): 1389-1400

Liu S, Hu RZ, Gao S, Feng CX, Coulson IM, Feng GY, Qi YQ, Yang YH, Yang CG and Tang L. 2012b. U-Pb zircon age, geochemical and Sr-Nd isotopic data as constraints on the petrogenesis and emplacement time of the Precambrian mafic dyke swarms in the North China Craton (NCC). Lithos, 140-141(1): 38-52

Liu S, Hu RZ, Gao S, Feng CX, Coulson IM, Feng GY, Qi YQ, Yang YH, Yang CG and Tang L. 2013. Zircon U-Pb age and Sr-Nd-Hf isotopic constraints on the age and origin of Triassic mafic dykes, Dalian area, Northeast China. International Geology Review, 55(2): 249-262

Liu YS, Hu ZC, Zong KQ, Gao CG, Gao S, Xu J and Chen HH. 2010b. Reappraisement and refinement of zircon U-Pb isotope and trace element analyses by LA-ICP-MS. Chinese Science Bulletin, 55(15): 1535-1546

Ludwig KR. 2003. User's manual for Isoplot/Ex, Version 3.00. A geochronological toolkit for Microsoft excel. Berkeley Geochronology Center Special Publication, 4: 1-70

Lugmair GW and Harti K. 1978. Lunar initial $^{143}Nd/^{144}Nd$: Differential evolution of the lunar crust and mantle. Earth and Planetary Science Letters, 39(3): 349-357

Mu BL and Yan GH. 1992. Geochemistry of Triassic alkaline or subalkaline igneous complexes in the Yanliao area and their significance. Acta Geologica Sinica, 66(2): 108-121 (in Chinese with English abstract)

Mu BL, Shao JA, Chu ZY, Yan GH and Qiao GS. 2001. Sm-Nd age and Sr, Nd isotopic characteristics of the Fanshan potassic alkaline ultramafite-syenite complex in Hebei province, China. Acta Petrologica Sinica, 17(3): 358-365 (in Chinese with English abstract)

Nelson DR, Chivas AR, Chapell BW and McCulloch MT. 1988. Geochemical and isotopic systematics in carbonatites and implications for the evolution of ocean-island sources. Geochimica et Cosmochimica Acta, 52(1): 1-17

Peng P, Zhai MG, Zhang HF and Guo JH. 2005. Geochronological constraints on the Palaeoproterozoic evolution of the North China Craton: SHRIMP zircon ages of different types of mafic dikes. International Geology Review, 47(5): 492-508

Peng P, Zhai MG, Guo JH, Kusky T and Zhao TP. 2007. Nature of mantle source contributions and crystal differentiation in the petrogenesis of the 1.78Ga mafic dykes in the central North China craton. Gondwana Research, 12(1): 29-46

Peng P, Zhai MG, Li Z, Wu FY and Hou QL. 2008. Neoproterozoic (~820Ma) mafic dyke swarms in the North China craton: Implication for a conjoint to the Rodinia supercontinent? Abstracts of 13th Gondwana Conference, Dali, China, 160-161

Peng P. 2010. Reconstruction and interpretation of giant mafic dyke swarms: A case study of 1.78Ga magmatism in the North China craton. Geological Society, London, Special Publication, 338: 163-178

Peng P, Guo JH, Zhai MG and Bleeker W. 2010. Paleoproterozoic gabbronoritic and granitic magmatism in the northern margin of the North China Craton: Evidence of crust-mantle interaction. Precambrian Research, 183(3): 635-659

Peng P, Bleeker W, Ernst RE, Söderlund U and McNicoll V. 2011a. U-Pb baddeleyite ages, distribution and geochemistry of 925Ma mafic dykes and 900Ma sills in the North China craton: Evidence for a Neoproterozoic mantle plume. Lithos, 127(1-2): 210-221

Peng P, Zhai MG, Li QL, Wu FY, Hou QL, Li Z, Li TS and Zhang YB. 2011b. Neoproterozoic (900Ma) Sariwon sills in North Korea: Geochronology, geochemistry and implications for the evolution of the south-eastern margin of the North China Craton. Gondwana Research, 20(1): 243-254

Qi L, Hu J and Grégoire DC. 2000. Determination of trace elements in granites by inductively coupled plasma mass spectrometry. Talanta, 51: 507-513

Qiu JX, Zeng GC and Li CN. 1993. The Alkaline Rocks in Qinling-Bashan Mountains. Beijing: Geological Publishing House, 1-176 (in Chinese with English abstract)

Ren FG, Li SB, Ding SY, Chen ZH, Zhao JN and Wu B. 1999. Alkaline magma activities, mineralization and formation model in Xiong Er Fault Basin. Geological Review, 45(S1): 660-667 (in Chinese with English abstract)

Rukhlov AS and Bell K. 2010. Geochronology of carbonatites from the Canadian and Baltic Shields, and the Canadian Cordillera: Clues to mantle evolution. Mineralogy and Petrology, 98(1-4): 11-54

Shao JA and Zhang LQ. 2002. Mesozoic dyke swarms in the north of North China. Acta Petrologica Sinica, 18(3): 312-318 (in Chinese with English abstract)

Shao JA, Zhang YB, Zhang IX, Mu B, Wang PY and Guo F. 2003. Early Mesozoic dyke swarms of carbonatites and lamprophyres in Datong area. Acta Petrologica Sinica, 19(1): 93-104 (in Chinese with English abstract)

Shao JA, Zhai MG, Zhang LQ and Li DM. 2005. Identification of 5 time-groups of dyke swarms in Shanxi-Hebei-Inner Mongolia Border area and its tectonic implications. Acta Geologica Sinica, 79(1): 56-67 (in Chinese with English abstract)

Steiger RH and Jäger E. 1977. Subcommission on geochronology: Convention on the use of decay constants in geo- and cosmochronology. Earth and Planetary Science Letters, 36(3): 359-362

Sun SS and McDonough WF. 1989. Chemical and isotopic systematics of oceanic basalts: Implication for mantle composition and processes. In: Saunders AD and Norry MJ (eds.). Magmatism in Oceanic Basins. Geological Society of London, Special Publication, 42(1): 313-345

Tarney J and Weaver BL. 1987. Geochemistry and petrogenesis of Early Proterozoic dyke swarms. In: Halls HC and Fahrig WC (eds.). Mafic Dyke Swarms. Geological Association of Canada, Special

Publication, 34: 81 – 93
Thompson RN, Smith PM, Gibson SA, Mattey DP and Dickin AP. 2002. Ankerite carbonatite from Swartbooisdrif, Namibia: The first evidence for magmatic ferrocarbonatite. Contribution to Mineralogy and Petrology, 143(3): 377 – 395
Verhulst A, Balaganskaya E, Kirnarsky Y and Demaiffe D. 2000. Petrological and geochemical (trace elements and Sr-Nd isotopes) characteristics of the Paleozoic Kovodor ultramafic, alkaline and carbonatite intrusion (Kola Peninsula, NW Russia). Lithos, 51(1 – 2): 1 – 25
Woolley AR and Kempe DRC. 1989. Carbonatites: Nomenclature, average chemical compositions, and element distribution. In: Bell K (ed.). Carbonatites: Genesis and Evolution. London: Unwin Hyman, 1 – 14
Wu LR. 1966. Research on the Alkaline Rock in Some Areas. Beijing: Science Press
Xu C, Campbell IH, Allen CM, Huang ZL, Qi L, Zhang H and Zhang GS. 2007. Flat rare earth element patterns as an indicator of cumulate processes in the Lesser Qinling carbonatites, China. Lithos, 95(3 – 4): 267 – 278
Xu C, Taylor RN, Kynicky J, Chakhmouradian AR, Song WL and Wang LJ. 2011. The origin of enriched mantle beneath North China block: Evidence from young carbonatites. Lithos, 127: 1 – 9
Yan GH, Mu BL, Zeng YS, Cai JH, Ren KX and Li FT. 2007. Igneous carbonatites in North China Craton: The temporal and spatial distribution, Sr and Nd isotopic characteristics and their geological significance. Geological Journal of China Universities, 13(3): 463 – 473 (in Chinese with English abstract)
Yang JH, Chung SL, Zhai MG and Zhou XH. 2004. Geochemical and Sr-Nd-Pb isotopic compositions of mafic dykes from the Jiaodong Peninsula, China: Evidence for vein-plus-peridotite melting in the lithospheric mantle. Lithos, 73: 156 – 160
Yang XK, Chao HX and Yang YH. 2006. Magmatismthermal action in Zijinshan area in the east part of the Ordos basin. The Abstract Collection of 2006 Symposium on Petrology and Geodynamics in China, 459 – 461 (in Chinese)
Ying JF and Zhou XH. 2001. Characterization of trace elements and Sr, Nd isotopes of carbonatites in the western Shandong Province. Bulletin of Mineralogy, Petrology and Geochemistry, 20(4): 309 – 311 (in Chinese with English abstract)
Ying JF, Zhou XH and Zhang HF. 2004. Geochemical and isotopic investigation of the Laiwu-Zibo carbonatites from western Shandong Province, China, and implications for their petrogenesis and enriched mantle source. Lithos, 75(3 – 4): 413 – 426
Yuan HL, Gao S, Liu XM, Li HM, Günther D and Wu FY. 2004. Accurate U-Pb age and trace element determinations of zircon by laser ablation-inductively coupled plasma mass spectrometry. Geostandards and Geoanalytical Research, 28(3): 353 – 370
Zhai MG, Fang HR, Yang JH and Miao LC. 2004. Large-scale cluster of cold deposits in east Shandong: Anorogenic metallogenesis. Earth Science Frontiers, 11(1): 95 – 98 (in Chinese with English abstract)
Zhang FQ. 2007. Lamprophyre invasion's effects on coal seam and its qualities in Tashan coal-field of Datong mining district. Shanxi Coal, 27(2): 17 – 20 (in Chinese with English abstract)
Zhang HF, Sun M, Zhou XH, Fan WM, Zhai MG and Yin JF. 2002. Mesozoic lithosphere destruction beneath the North China Craton: Evidence from major-, traceelement and Sr-Nd-Pb isotope studies of Fangcheng basalts. Contribution to Mineralogy and Petrology, 144(2): 241 – 253
Zhang HF, Sun M, Zhou XH and Ying JF. 2005. Geochemical constraints on the origin of Mesozoic alkaline intrusive complexes from the North China Craton and tectonic implications. Lithos, 81(1 – 4): 297 – 317
Zhao GC, Wilde SA, Cawood PA and Sun M. 2001. Archean blocks and their boundaries in the North China Craton: Lithological, geochemical, structural and *P-T* path constraints and tectonic evolution. Precambrian Research, 107(1 – 2): 45 – 73
Zhao JX and McCulloch MT. 1993. Melting of a subduction-modified continental lithospheric, mantle: Evidence from Late Proterozoic mafic dyke swarms, in central Australia. Geology, 21(5): 463 – 466
Zheng YF. 2012. Metamorphic chemical geodynamics in continental subduction zones. Chemical Geology, 328: 5 – 48
Zou HB, Zindler A, Xu XS and Qi Q. 2000. Major, trace element, and Nd, Sr and Pb isotope studies of Cenozoic basalts in SE China: mantle sources, regional variations and tectonic significance. Chemical Geology, 171: 33 – 47

附中文参考文献

白鸽，袁忠信. 1985. 碳酸岩地质及其矿产. 中国地质科学院矿床地质研究所所刊,第1号:99 – 175
范宏瑞，胡芳芳，陈福坤，杨奎锋，王凯怡. 2006. 白云鄂博超大型REE-Nb-Fe 矿区碳酸岩墙的侵位年龄-兼答 Le Bas 博士的质疑. 岩石学报，22(2)：519 – 520
冯光英，刘燊，钟宏，贾大成，齐有强，王涛，杨毓红. 2010. 吉林晚古生代榆木川基性岩的地球化学特征及其岩石成因. 地球化学，39(5)：427 – 438
刘燊，胡瑞忠，赵军红，冯彩霞，钟宏，曹建劲，史丹妮. 2005. 胶北晚中生代煌斑岩的岩石地球化学特征及其成因研究. 岩石学报，21(3)：947 – 958
刘燊，胡瑞忠，冯光英，杨毓红，冯彩霞，齐有强，王涛. 2010. 华北克拉通中生代以来基性岩墙群的分布和研究意义. 地质通报，29(2 – 3)：259 – 267
牟保磊,邵济安,储著银,阎国翰,乔广生. 2001. 河北矾山钾质碱性岩-正长岩杂岩体 Sm-Nd 和 Sr、Nd、Pb 同位素特征. 岩石学报,17(3)：358 – 365
邱家骧,曾广策,李昌年. 1993. 秦巴碱性岩. 北京:地质出版社,1 – 176
任富根，李双保，丁士应，陈志宏，赵嘉农，吴冰. 1999. 熊耳裂陷印支期碱性岩浆活动成矿作用、生成模式. 地质论评，45(S1)：659 – 667
邵济安，张履桥. 2002. 华北北部中生代岩墙群. 地质学报，18(3)：312 – 318
邵济安，张永北，张履桥，牟保平，王佩瑛，郭锋. 2003. 大同地区早中生代煌斑岩-碳酸岩岩墙群. 岩石学报，19(1)：93 – 104
邵济安，翟明国，张履桥，李大明. 2005. 晋冀蒙交界地区五期岩墙群的界定及其构造意义. 地质学报，79(1)：56 – 67
吴利仁. 1966. 若干地区碱性岩研究. 北京:科学出版社
阎国翰，牟保磊，曾贻善，蔡剑辉，任康绪，李凤棠. 2007. 华北克拉通火成碳酸岩时空分布和锶钕同位素特征及其地质意义. 高校地质学报，13(3)：463 – 473
杨兴科,晁会霞,杨永恒. 2006. 鄂尔多斯盆地东部紫金山一带岩浆-热力作用问题. 2006 年全国岩石学与地球动力学研讨会论文摘要,459 – 461
英基丰，周新化. 2001. 鲁西地区中生代碳酸岩类的微量元素和锶、钕同位素组成特征. 矿物岩石地球化学通报，20(4)：309 – 311
翟明国,范宏瑞,杨进辉,苗来成. 2004. 非造山带型金矿 – 胶东型金矿的陆内成矿作用. 地学前缘,11(1)：95 – 98
张富强. 2007. 大同塔山井田煌斑岩侵入对煤层煤质的影响. 山西煤炭，27(2)：17 – 20